

## Forum Review

# *In Vitro* and *In Vivo* Measurement of pH and Thiols by EPR-Based Techniques

VALERY V. KHRAMTSOV,<sup>1,2</sup> IGOR A. GRIGOR'EV,<sup>3</sup>  
MARGARET A. FOSTER,<sup>4</sup> and DAVID J. LURIE<sup>4</sup>

### ABSTRACT

*In vitro* and *in vivo* measurements of pH and thiols provide critical information on physiology and pathophysiology of living organisms, particularly related to oxidative stress. Stable nitroxides of imidazoline and imidazolidine types provide the unique possibility of measuring local values of pH and glutathione content in various biological systems, including *in vivo* studies. The basis for these applications is the observation of specific chemical reactions of these nitroxides with protons or thiols, followed by significant changes in the electron paramagnetic resonance (EPR) spectra of these probes, measured by low-frequency EPR techniques. The applications of some newly developed pH and SH probes in model systems of pharmacological interest, biological fluids, tissues, and cells as well as *in vivo* studies in isolated hearts and in the gut of living animals are discussed. *Antioxid. Redox Signal.* 6, 667–676.

### INTRODUCTION

LOCAL pH AND THIOL CONTENT, particularly glutathione (GSH) concentration, are among the most important parameters in the biochemistry of living organisms. Many of the vital activities of cells depend on the pH inside cellular organelles, transmembrane pH gradients, and the pH at the surface of membranes or proteins (60). Likewise, the roles of vital SH groups and intracellular GSH, particularly in the maintenance of intracellular “redox state,” are also widely appreciated (65). In certain stress conditions, *e.g.*, inflammation, high exercise levels, interruption of normal blood supply, or biochemical shock, the body's ability to regulate its pH and GSH content, at least locally, may be compromised. Tissue acidosis and redox state are dominant factors in inflammation (4, 27, 72, 73) and in tumors (24, 26, 45, 68) and after ischemia (28, 70, 79). In addition, the delivery, absorption, and pharmacological effectiveness of drugs can be altered by changing the pH and redox state of their local environment (1, 57, 69, 76). It can be seen therefore that pH and

GSH measurement *in vivo* may be of considerable clinical relevance.

Recently Kuppusamy *et al.* (45) used indirect evaluation of GSH content by *in vivo* electron paramagnetic resonance (EPR) spectroscopy and imaging to demonstrate a central role of GSH in the reduction of the nitroxide in a murine tumor model. However, up to now there is no direct, non-invasive method for GSH detection in living tissues.

As for *in vivo* pH measurements, <sup>31</sup>P-nuclear magnetic resonance (NMR) has proven to be the most suitable non-invasive approach. Nevertheless, pH assessment using <sup>31</sup>P-NMR and inorganic phosphate has its own limitations, including lack of resolution (about 0.2–0.3 units and even less at lower pH), the fact that inorganic phosphate concentrations vary with metabolism and ischemia, and its chemical shift depends on ionic strength (19, 46, 62, 67). Because of these problems, exogenous pH probes are being designed for <sup>31</sup>P-NMR spectroscopy (11, 62) to improve detection of acidosis in isolated perfused organs. In addition, several NMR approaches for pH detection utilizing <sup>1</sup>H-NMR (71), <sup>19</sup>F-NMR

<sup>1</sup>Dorothy M. Davis Heart & Lung Research Institute, The Ohio State University, Columbus, OH.

Institutes of <sup>2</sup>Chemical Kinetics & Combustion and <sup>3</sup>Organic Chemistry, Novosibirsk, Russia.

<sup>4</sup>Department of Biomedical Physics and Bioengineering, University of Aberdeen, Aberdeen, United Kingdom.

(61), and contrast-enhanced magnetic resonance imaging (63) have been reported. Recently developed EPR-based spectroscopic and imaging approaches, in combination with function-directed pH- and SH-sensitive spin probes (7, 15, 26, 31, 32, 38), open another unique possibility for following early stages in the changes of body chemistry *in vivo* that are associated with certain stressful or pathological conditions. The pH-sensitive nitroxides, since they are exogenous probes, have certain advantages over exogenous NMR probes, due to the much higher sensitivity of EPR.

### *In vivo EPR-based spectroscopy and imaging*

Despite formidable technical problems, significant progress has been made in the development of *in vivo* EPR techniques during the last decade. Low-frequency L-band EPR spectrometers, designed to decrease non-resonant losses and increase depth of microwave penetration, have become commercially available. Moreover, even lower-frequency (down to 300 MHz) home-made radiofrequency-EPR spectrometers, as well as instrumentation for spatial and spectral-spatial EPR imaging of radicals, have been constructed in several laboratories and have effectively been used for free radical spectroscopy and imaging (5, 16, 18, 23, 30, 38, 42, 47, 66). Along with the progress in low-frequency radiofrequency-EPR, other techniques such as longitudinally detected electron spin resonance (LODESR) (58), proton electron double-resonance imaging (PEDRI), and dynamic nuclear polarization (DNP) (49, 51) have been developed for *in vivo* applications. The EPR and PEDRI techniques have been used to image free radicals in living tissues, including heart (39, 43, 44, 80) and stomach (15, 17, 38) in rats. However, their potential is still far from maximally defined, in part, because of the need for development of new specific function-directed spin probes.

### *Molecular pH-sensitive spin probes*

The possibility of accurate determination of pH values by EPR is based on early findings that EPR spectra parameters of stable nitroxides of the imidazoline and imidazolidine types, namely, the hyperfine (hf) splitting constant,  $a_N$ , and the  $g$ -factor, depend on the pH of the surrounding solution (29, 33). It is possible to use the  $a_N$  constant as a sensitive indicator of pH in the range of about 1.5 pH units above and below the  $pK$  value of the nitroxides. Here we discuss both the current biological applications of spin pH probes and the development of new probes that are particularly designed for *in vivo* studies, namely, with higher spectral sensitivity, stability towards reduction, and usefulness for pH monitoring in physiological range of pH, and for potential intracellular targeting of the probe.

### *Molecular SH-sensitive spin probes*

The EPR method for SH group detection is based on the use of thiol-sensitive paramagnetic disulfides (35, 37), which participate in reactions of thiol-disulfide exchange, similar to Ellman's reagent, commonly used for thiol determination by an optical method (8). Here we discuss the applications of two different paramagnetic SH probes, particularly with respect to the possibility for *in vivo* detection of thiols.

## SPIN pH PROBES

### *Manifestation of pH effect in the EPR spectra of imidazoline and imidazolidine nitroxides*

The ionizable molecular pH probes have spectroscopically distinguishable protonated ( $RH^+$ ) and unprotonated ( $R$ ) forms with their relative fraction depending on pH, namely,  $[RH^+]/[R] = [H^+]/K_a$ , where  $K_a$  is the equilibrium constant of the reaction of probe protonation or dissociation. Figure 1 illustrates the EPR spectra of a spin probe of the imidazoline type, R1 (Scheme 1), and its deuterated analog, R1\*, in aqueous solutions,  $pH \approx pK$  ( $pK = -\log K_a$ ), at various microwave frequencies. The presence of two forms of the probes with different hf splittings ( $\Delta a_N \approx 1$  G) and  $g$ -factors ( $\Delta g \approx 0.002$ ) is more evident for the substituted R1\* compound because of narrow lines (Fig. 1a\*–c\*). Note that the contribution of the  $g$ -factor is significant only at higher frequency (X-band, 9.9 GHz), resulting in the asymmetry of the pH effect for low- and high-field EPR spectral components (Fig. 1a and a\*), while the L-band EPR spectrum (1.2 GHz) demonstrates a very symmetric spectral pattern (Fig. 1b and b\*). The asym-

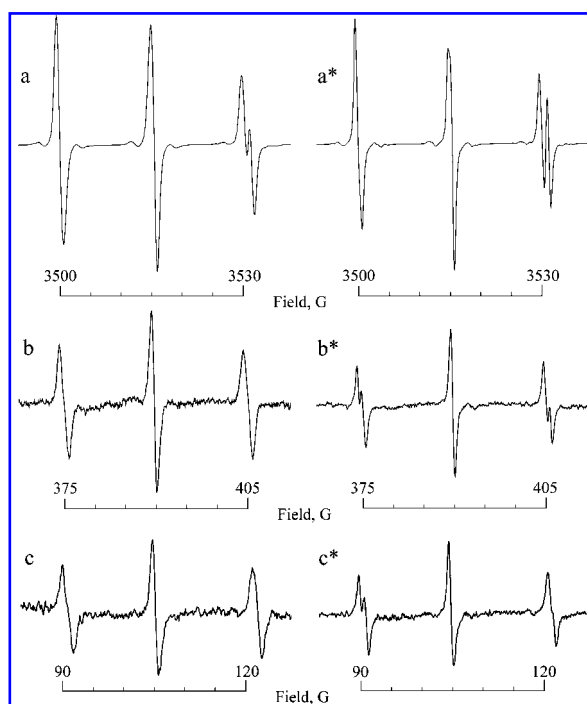
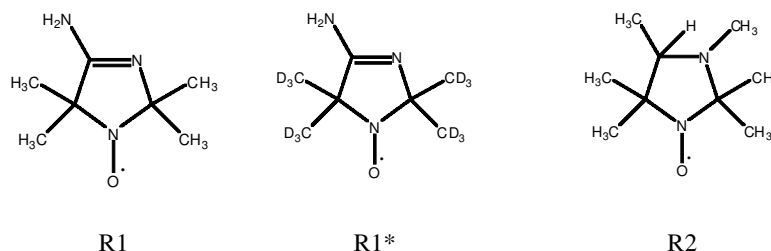


**FIG. 1.** The EPR spectra of an aqueous solutions of 0.5 mM nitroxides R1 and R1\* at pH 6.1 measured at 9.9 GHz (a and a\*), 1.2 GHz (b and b\*), and 300 MHz (c and c\*). The experimental volumes were 50  $\mu$ l, 0.5 ml, and 20 ml, respectively. The spectra were detected with an X-band Bruker EMX spectrometer (Bruker Instruments, Karlsruhe, Germany) and home-built L-band and 300 MHz spectrometers (EPR Center at The Ohio State University, Columbus, OH, U.S.A.) using the same modulation amplitude (0.2 G) and detection time (2 min) for the sensitivity comparison. EPR spectra of the substituted radical (\*) are depicted at two times lower scale and show about a twofold increase in signal-to-noise ratio due to decrease in the linewidths.



**SCHEME 1.** Chemical structures of the imidazoline radical, R1; its deuterio-substituted analog, R1\*; and the imidazolidine radical, R2.

metry of the spectra at lower frequency (300 MHz, Fig. 1c and c\*) has a completely different origin and is due to the Breit–Rabi effect (9). The value of the  $pK$  of the radical is the main characteristic of the “molecular pH meter” that determines the range of pH sensitivity to be about 3 pH units, centered on the  $pK$ . The pH determination may be done from calculation of  $[RH^+]/[R]$  ratio by spectra computer simulation or by using titration curve for certain spectral parameters, *e.g.*, hf splitting or spectral peak intensities ratio (32). The pH dependence of hf splitting,  $a_N$ , measured as a distance between low- and central field components, was proven to provide a simple and sensitive approach for pH measurement by X-band EPR spectroscopy (32). However, using hf splitting for pH determination by L-band and 300 MHz spectroscopy is less preferable because of the narrow range of its pH sensitivity (Fig. 2c, squares). Therefore application of peak intensity ratio or computer analysis of spectral shape based on superposition of two triplet spectra of protonated and unprotonated forms of the radical is recommended for pH determination by these EPR techniques. Substituted probes have an advantage in spectral resolution and signal-to-noise ratio while being less available and more costly. Interestingly, both signal-to-noise ratio and the range of pH sensitivity of hf splitting can be significantly increased by spectra detection at high modulation amplitude (Fig. 2). Indeed, improvement in signal-to-noise ratio due to application of the substituted radical R1\* compared with R1 is significant only at lower modulation amplitude (about two times at 0.2 G modulation, Fig. 1), while it becomes less significant at higher modulation (about 1.5 times at 0.5 G modulation) and does not improve signal-to-noise at a modulation amplitude larger than 1 G. On the other hand, the measurement of EPR spectra at a high modulation amplitude of 2 G results in about two and four times signal-to-noise improvement compared with L-band EPR spectra detected at 0.5 G and 0.2 G modulation, respectively (Fig. 2a and b). This enhancement in the signal-to-noise is by the cost of broadening of the spectral lines and corresponding loss of spectral resolution. Fortunately, it also results in smoothing the pH titration curve for hf splitting,  $a_N$  (see Fig. 2b), making this parameter a highly sensitive pH marker. The methodical approach described could be important for applications *in vivo* where fundamental sensitivity is much lower.

Up to the present time we have developed a wide set of pH-sensitive nitroxides, with differing ranges of pH sensitivity, labeling groups, and lipophilicity (31, 32).

### In vitro applications of spin pH probes

Biological EPR applications at X-band are mostly limited by *in vitro* or *ex vivo* studies because of high non-resonant absorption of the excitation frequency by aqueous samples. Therefore spin pH probes have been used for the studies of the samples whose volume does not exceed 200  $\mu$ l. Monitoring transfer of protons across lipid bilayers of liposomes caused by a transmembrane pH gradient had been one of the first applications of the pH measurement by EPR (2, 34). Interestingly, the observation of the different rates of proton transport across phospholipid membranes upon the establishment of the gradient of different acids (34) allowed us to measure the membrane permeability coefficient for the undissociated forms of the acids,  $p_{HX}$ , including that for

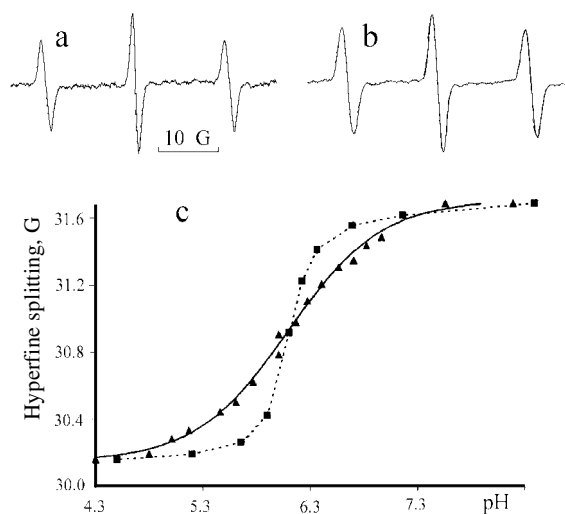


**FIG. 2.** The L-band EPR spectra (a and b) and pH dependence of hf splitting (c) for the radical R1 measured at different modulation amplitudes. The EPR spectra of the 0.5 mM aqueous solutions of the radical R1 were detected at pH 6.1, modulation amplitude 0.5 G (a) or 2 G (b), microwave power 10 mW, sweep widths 50 G, center field 389 G, acquisition time 56 s, and time constant 0.1 s. Spectrum b is depicted at two times lower scale and shows 2.1 and 4.2 times increase in signal-to-noise ratio compared with Spectrum a and the spectrum shown in Fig. 1b, respectively. c: The pH dependence of hf splitting for the radical R1 was measured as the distance between low- and high-field components of L-band EPR spectra obtained at modulation amplitude 0.5 G (■) and 2 G (▲).

$\text{HNO}_3$  ( $\text{p}K = -1.62$ ;  $\text{p}K_{\text{HX}} = 1.4 \times 10^{-4} \text{ cm/s}$ ). Because of the importance of  $\text{NO}_x$  species in cellular biology, and discussion of nonenzymatic nitric oxide formation from nitrite in acidic environments or upon ischemic or metabolic acidosis (64, 79), there appears to be significant interest in the studies of nitrite transfer through the biomembranes *via* transmembrane diffusion of the undissociated acid  $\text{HNO}_2$  ( $\text{p}K_{\text{HNO}_2} = 3.3$ ). This transport facilitates proton transfer across the biomembrane and therefore can be studied using membrane-impermeable pH-sensitive nitroxides (2, 3, 34).

The other *in vitro* applications of spin pH probes include studies of water-in-oil ointments (41), proteins and proteinaceous matrix (10, 36), and biodegradable polymers and phospholipid membranes (10, 36, 53, 54). Recently Kroll *et al.* applied spin pH probes for non-invasive direct and depth-specific measurement of pH values within rat and human skin (the latter obtained from cosmetic surgery) (42) to study influence of drug treatment on the microacidity.

### In vivo applications of spin pH probes

Spin pH probes offer a unique opportunity for non-invasive pH measurement in living animals using low-field EPR-based techniques [for reviews, see Khramtsov *et al.* (38) and Mäder (52)]. L-band EPR spectroscopy (1.2 GHz) was shown to be a valuable tool for *in vivo* monitoring of biodegradable drug delivery systems (55) and pH measurement in mice (17). Recently we applied spin pH probes for the studies in living rats (15, 38) using LODESR (58) and field-cycled DNP (48) with its imaging analogue, field-cycled PEDRI (FC-PEDRI) (49, 50), operating at an EPR frequency as low as 120 MHz.

Figure 3 displays an FC-PEDRI image from a living rat with gastric infusion of the probe R2 (Scheme 1) in deionized

water (15). The image obtained with FC-PEDRI is used to determine the probe localization, supporting its presence in the stomach, as shown in Fig. 3d. The EPR-based spectroscopy component of FC-PEDRI and the LODESR spectra provide information on the environmental acidity (Fig. 4). The changes in the distance between low- and high-field components of the spectra, after addition of 0.1 M sodium bicarbonate, clearly demonstrate the action of this particular antacid. Oral administration of some of the pH-sensitive radicals has been found to improve the ability of the probe to stay in the stomach for ~1 h, in the radical form, while more hydrophobic radicals tend to be absorbed through the membranes of the stomach walls, therefore losing the EPR signal (15, 38).

Figure 5 demonstrates a typical EPR spectrum of the pH probe, R1, in the isolated working heart (39), located directly in the resonator of the L-band EPR spectrometer. The EPR spectrum is significantly affected by ischemic acidosis and corresponds to pH 6.5 after 5 min of ischemia. This result is in agreement with the data observed by a  $^{31}\text{P}$ -NMR technique that demonstrates similar acidosis at this time point (79). Note that the reduction of the radical into diamagnetic products (mostly to corresponding hydroxylamine) limits its de-

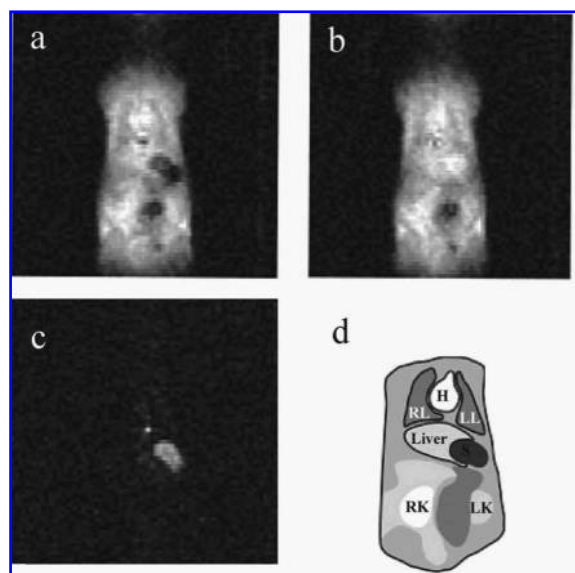


**FIG. 3.** FC-PEDRI image of a rat intubated 30 min previously with 3.5 ml of 7 mM R2 solution: obtained (a) with ESR irradiation off and (b) with ESR irradiation on. c: The difference between (a) and (b). d: The diagram demonstrates the anatomy. RL and LL, right and left lung, respectively; H, heart; S, stomach; RK and LK, right and left kidney, respectively.

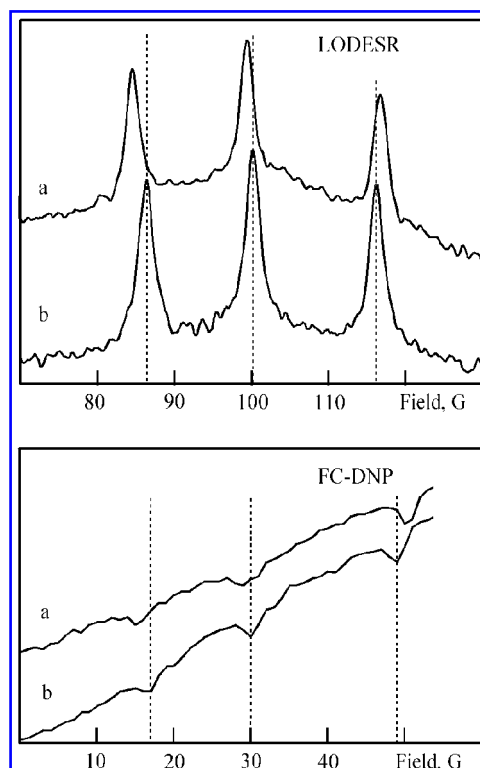


**FIG. 4.** LODESR (304 MHz; top panel) and FC-DNP (119 MHz; bottom panel) spectra from rats given 3.5 ml of 7 mM R2 solution in 0.1 M  $\text{NaHCO}_3$  solution (Spectrum a) or in deionized water (Spectrum b). The LODESR spectra were collected approximately 10 min and the FC-DNP spectra 15 min after dosing. In addition to the narrowing of the splitting arising from acidification of the agent when given in water alone, there is a small difference in splitting between the two techniques, arising from the different measurement frequencies. In each case a dotted line is extended from each peak of Spectrum b to aid the eye.

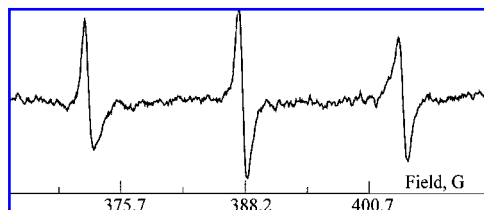


**FIG. 5.** L-band EPR spectrum of R1 (see Scheme 2) in isolated perfused rat heart (infused 1 min prior to ischemia through a side arm to achieve final radical concentration of about 50  $\mu\text{M}$ ) after 5 min of ischemia. The spectrum is detected at a modulation amplitude of 0.5 G and shows superposition of two forms of the radical (protonated and unprotonated) resulting in disturbance of low- and high-field components and inequality of spectral peak intensities, as well as pH-dependent changes in the distance between these components. EPR-determined pH =  $6.5 \pm 0.1$ .

tection by EPR for the time window of about 20 min after a single infusion of the R1 as a bolus. Recently we described the synthesis of new series of pH-sensitive nitroxides with increased stability towards reduction due to the substitution of methyl groups in the vicinity of the -NO fragment by more bulky ethyl groups (40).

Intracellular and extracellular targeting is another important direction in the development and biological applications of spin pH probes. For this purpose we proposed synthesis of pH-sensitive nitroxides with ester groups for its intracellular targeting (74). Similar to other molecular probes with ester groups, *e.g.*, fluorescent probes (20), these nitroxides will

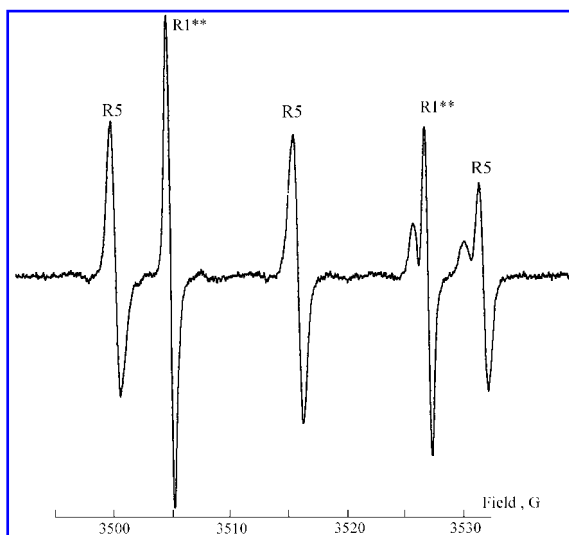
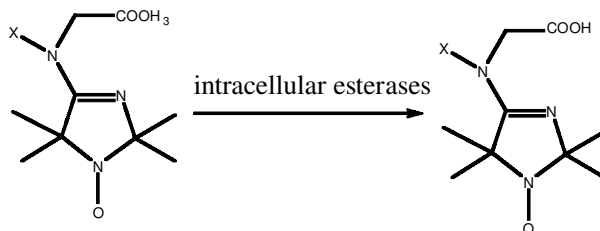


**FIG. 6.** X-band EPR spectrum of the mixture of the radicals R5 and  $^{15}\text{N}$ -1 substituted radical R1 in 0.1 mM sodium phosphate buffer, pH 6.7. The doublet spectrum of the  $^{15}\text{N}$  isotopically substituted probe, R1\*\*, and triplet spectrum of the R5 radical with the  $^{14}\text{N}$ -O fragment do not overlap, allowing simultaneous application of these spin probes for pH determination.



**SCHEME 2.** Expected hydrolysis of the ester derivatives of the imidazoline radicals, R3 (X = Me) and R4 (X = Ph), into the corresponding carboxy derivatives, R5 and R6, inside the cells. This strategy maximizes the potential for intracellular localization of the spin pH probes.

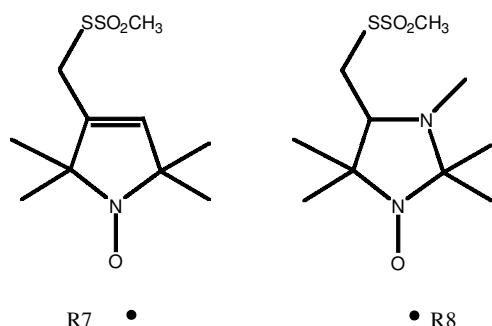
presumably accumulate intracellularly after hydrolysis of the ester bond by endogenous intracellular esterases (Scheme 2). This is supported by preliminary data obtained with carboxy-derivative R5 (Scheme 2, X = Me). The EPR-measured pK of carboxyl group of R5 was found to be as low as 2.5, resulting in ionic character of this compound at physiological pH and its low transmembrane permeability through the bilayer of phosphatidylcholine liposomes. Note that application of an intracellular targeted probe with the  $^{14}\text{N}$ -O fragment and an extracellular membrane-impermeable probe with the  $^{15}\text{N}$ -O fragment provides possibility to detect both signals because their EPR spectra do not overlap (Fig. 6) and, therefore, opens the possibility of simultaneous detection of intracellular and extracellular pH.

## SPIN SH PROBES

### *Basis of the method of spin SH probes*

The usefulness of the application of the paramagnetic disulfide, methanethiosulfonate spin label R7 (Scheme 3), in assaying reactive thiol groups in proteins was first demonstrated by Berliner *et al.* (6). The approach utilizes cysteine-directed spin labeling using this highly reactive thiol-specific reagent. One of the disadvantages of the approach is the requirement of the purification of the labeled protein from the unreacted radical. The other obstacle for thiol detection using disulfide R7 is insensitivity of its EPR spectrum towards the reaction with low-molecular-weight thiols.

The thiol-specific reagent R7 was found to be the most commonly used label in site-directed spin labeling, a powerful tool for monitoring the structure and dynamics of both soluble and membrane proteins (25). Recently a new methanesulfonate spin label, R8 (Scheme 3), with a pH-sensitive imidazolidine radical fragment (*cf.* R8 with imidazolidine radical R2, Scheme 1) has been synthesized (21). The reaction of the R8 with SH group of human serum albumin results in the formation of a pH-sensitive spin-labeled protein (Fig. 7), showing the ability of the label both to modify SH



**SCHEME 3.** Chemical structures of the methanethiosulfonate spin label R7 (6) and R8 (21).

groups of the proteins and to report local pH in the site of modification. To our opinion, the application of pH-sensitive thiol-specific reagents in site-directed spin labeling could provide new information on local polarity and electrostatic properties within the protein matrix.

The more direct EPR method for the detection of both low- and high-molecular-weight thiols is based on the application of biradical disulfide reagents, RSSR, where R represent an imidazoline (35) or imidazolidine (37) radical fragment (Scheme 4). These paramagnetic disulfides react with thiols, splitting the disulfide bond, resulting in characteristic changes of the EPR spectra (Figs. 8 and 9). The measurement of relative changes of the intensities of monoradical (Im) or biradical (Ib) components allows quantitative determination of GSH. The significant difference in the reactivity of the im-

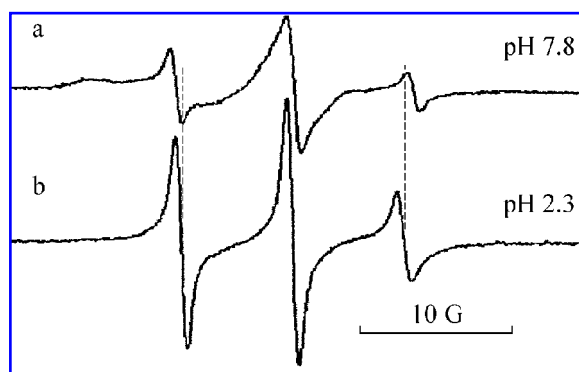


**FIG. 7.** X-band EPR spectra of human serum albumin solution labeled with the label R8 [modification degree 0.96, protein concentration 50  $\mu\text{M}$ ; for labeling procedure see Khramtsov *et al.* (37)]. The observed pH-dependent spectral changes were reversible. Spectrum a represents the unprotonated form of the radical bound to protein (pH 7.8,  $a_N = 15.80$  G), and Spectrum b is characteristic for the protonated form (pH 2.3,  $a_N = 14.60$  G). The higher mobility of the protonated label bound to albumin may indicate its weaker association with the protein surface due to electrostatic repulsion of the positively charged radical fragment from the surface of positive electric potential [ $\phi \sim 30$  mV for human serum albumin at pH from 2.5 to 3 (36)]. The dotted lines are extended from low- and high-field components of Spectrum b to aid the eye.

**TABLE 1.** BIMOLECULAR RATE CONSTANTS AND CHARACTERISTIC REACTION TIME OF THE DISULFIDE BIRADICALS WITH GSH (31)

	$k_f$ with GSH at pH 7.0	$\tau \sim 1/k_f[\text{GSH}]$ at 1 mM GSH
$\text{R}_1\text{S-SR}_1$	$\sim 5 \times 10^3 \text{ M}^{-1} \text{ s}^{-1}$	0.2 s
$\text{R}_2\text{S-SR}_2$	$0.26 \text{ M}^{-1} \text{ s}^{-1}$	60 min

idazoline biradical,  $\text{R}_1\text{SSR}_1$ , and the imidazolidine biradical,  $\text{R}_2\text{SSR}_2$ , with thiols (Table 1) allows different experimental approaches for their application.

The fast reactive  $\text{R}_1\text{SSR}_1$  probe can be applied only in a “static” approach, which measures the fraction of the biradical split by the reaction with thiols. This approach unambiguously requires an excess of the probe over thiols and results in consumption of total thiols under measurement, therefore interfering with normal cell function and making it impossible for *in vivo* use. The slow reactive  $\text{R}_2\text{S-SR}_2$  probe, however, can be applied in both “static” and “kinetic” approaches. The latter measures the rate of the biradical disulfide bond splitting, and therefore insignificant fraction of thiols may be consumed during measurement.

The biradical  $\text{R}_1\text{S-SR}_1$  has been used to measure GSH content in blood cells (14, 35), Chinese hamster ovary cells (75), murine neuroblastoma and malignant melanoma cells (12), and tumor HeLa cells (13). Noninvasive measurement of intracellular GSH using disulfide SH probes is based on the dominant contribution of GSH in the reaction with biradicals, fast diffusion of the probe across the cellular membrane, and its comparatively low reduction. The sensitivity of the method is sufficiently high to perform the measurements in very few ( $\sim 100$ ) cells (75). EPR studies of thiols in human and rat blood have demonstrated an increased level of oxidized GSH in the plasma under oxidative stress conditions (14, 77). The EPR assay for measurement of thiols in the blood is a sensitive and convenient method for fast analysis, which does not require complicated procedures for sample preparation. Nohl *et al.* (59) have applied the biradical,  $\text{R}_1\text{SSR}_1$ , for determination of thiol levels in isolated perfused hearts during ischemia/reperfusion. The authors measured release of the monoradicals into the perfusate, due to the reaction of the biradical disulfide with tissue thiols, and observed a decrease in the GSH level following ischemia/reperfusion.

The disadvantages of the “static” approach are the requirement of excessive amounts of the label,  $\text{RS-SR}$ , over thiols, resulting in the “consumption” of critical SH groups and subsequent irreversible damage to the system. The application of the “kinetic” approach using the disulfide reagent,  $\text{R}_2\text{S-SR}_2$ , allows a decrease of label concentration and therefore minimizes its possible toxicity. For the first time the application of the  $\text{R}_2\text{S-SR}_2$  in combination with “kinetic” approach provides a tool that can be used for real-time measurements of the GSH redox state that is not damaging to the tissue being studied. The reasonable value of characteristic time,  $\tau$ , for the reaction of the biradical  $\text{R}_2\text{S-SR}_2$  with GSH at physiological GSH concentrations and neutral pH (see Table 1 and Fig. 9) allows its application *in vivo*. Indeed, Fig. 9 demonstrates a convenient time window for the biradical,  $\text{R}_2\text{S-SR}_2$ , reaction

SCHEME 4. Chemical structures of the disulfide biradical labels.

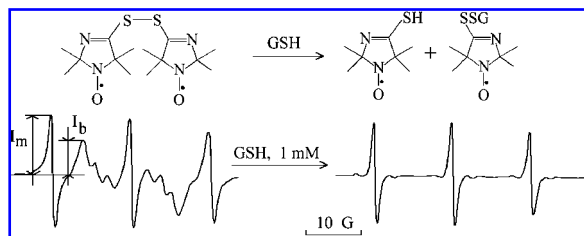
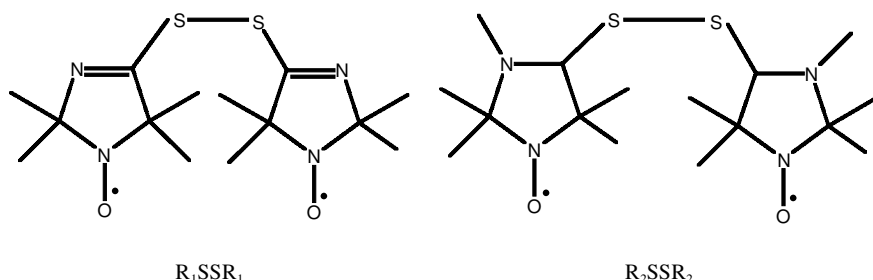


FIG. 8. X-band EPR spectrum of 0.1 mM solution of  $R_1S-SR_1$  in 0.1 M phosphate-buffered saline buffer, pH 7.4, and its transformation upon treatment with GSH, and the scheme of the corresponding reaction of thiol-disulfide exchange responsible for observed spectral changes. The measurement of relative changes of the intensities of monoradical ( $I_m$ ) or biradical ( $I_b$ ) components allows quantitative determination of GSH.

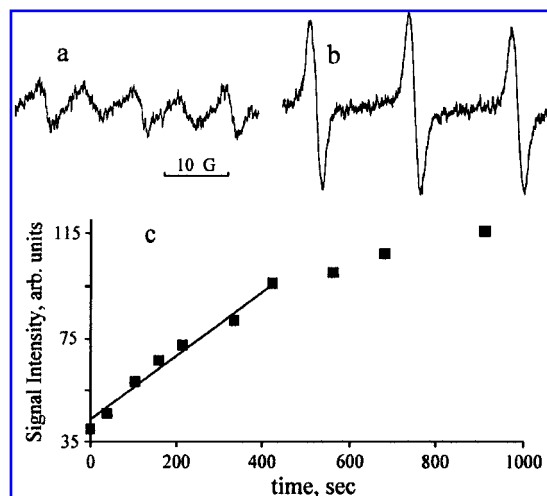


FIG. 9. L-band EPR spectra of 100  $\mu$ l of blood taken from a Sprague-Dawley rat measured 10 s (a) and 700 s (b) after addition of 5  $\mu$ l of the biradical  $R_2SSR_2$  (final concentration of the label 50  $\mu$ M, acquisition time 10.5 s). c: The time dependence of the low-field component of the spectra allows linear approximation in the time range less than 400 s, which can be used for estimation of GSH concentration.

with GSH in untreated rat blood, as well as its relative stability towards reduction (less than 10% of the radical was reduced during a 15-min incubation in blood). Note that the  $R_2S-SR_2$  radical freely penetrates cellular membranes [lipophilicity coefficient = 240 (37)], reacting preferably with intracellular GSH, while the reaction with protein thiols seems to be very slow, *e.g.*, rates constants for the reaction of  $R_2S-SR_2$  with SH groups of human serum albumin and hemoglobin are hundreds of times less compared with that for GSH (37). Therefore, taking into account the dominant contribution of GSH in the experimental kinetics shown in Fig. 9, we calculated the GSH concentration in rat whole blood (located mostly in the erythrocytes) to be equal to  $0.95 \pm 0.2$  mM, in reasonable agreement with literature data and with the data obtained by optical methods (8, 22).

Recently, we applied low, nontoxic concentrations of  $R_2SSR_2$  and the kinetic EPR approach for a demonstration of increased GSH oxidation in an animal model of stress-sensitive arterial hypertension (56, 78). It was found that the concentration of GSH in blood of the hypertensive rats is significantly lower compared with that of normotensive Wistar rats. These data support an elevated thiol oxidation and free radical mechanism involved in the pathogenesis of this animal model of hypertension (52, 78).

The possibility of applying the kinetic EPR approach *in vivo*, using a redox-sensitive nitroxide, was recently demonstrated by Kuppusamy *et al.* (45), allowing redox mapping of a tumor in "radiation-induced fibrosarcoma (RIF-1)-tumor bearing" mice. The authors showed a central role of GSH in the reduction of the nitroxide. The GSH level was significantly higher in the tumor tissue compared with normal tissue (26). However, it is necessary to note that the applied probe is not GSH-specific and is not even thiol-specific, but rather sensitive to any reducing compound. Therefore, application of an SH-sensitive probe, the biradical  $R_2SSR_2$ , which entails a similar kinetic EPR approach, might provide even more specific information.

## CONCLUSIONS

It is apparent that functional spin probes with EPR spectra sensitivity to concentrations of physiologically relevant species have become an important field of biomedical EPR applications. In this respect imidazoline and imidazolidine nitroxides were found to be the most promising probes providing the possibility to measure critical intracellular parameters, namely, local concentrations of protons (pH) and thiols.

## ACKNOWLEDGMENTS

The authors thank Dr. Govindasamy Ilangoan, Sergey Petryakov, and Valerie Wright for technical assistance. This work was partly supported by grants from The Royal Society (London), INTAS (No. 99-1086), and NIH grants NHLB 53333 and EB 03519.

## ABBREVIATIONS

DNP, dynamic nuclear polarization; EPR, electron paramagnetic resonance; FC-PEDRI, field-cycled proton electron double-resonance imaging; GSH, glutathione; hf, hyperfine; LODESR, longitudinally detected electron spin resonance; NMR, nuclear magnetic resonance; PEDRI, proton electron double-resonance imaging.

## REFERENCES

- Asokan A and Cho MJ. Exploitation of intracellular pH gradients in the cellular delivery of macromolecules. *J Pharm Sci* 91: 903-913, 2002.
- Balakirev M. and Khramtsov V. New pH-sensitive aminoxyls—application to the study of biomembrane transport processes. *J Chem Soc Perkin Trans 2*: 2157-2160, 1993.
- Balakirev MYu, Khramtsov VV, Berezina TA, Martin VV, and Volodarsky LB. The synthesis of amidine derivatives of imidazoline nitroxides—a new series of pH-sensitive spin probes and labels. *Synthesis* 1223-1225, 1992.
- Beeh KM, Beier J, Haas IC, Kornmann O, Micke P, and Buhl R. Glutathione deficiency of the lower respiratory tract in patients with idiopathic pulmonary fibrosis. *Eur Respir J* 19: 1119-1123, 2002.
- Berliner LJ and Fujii H. Magnetic resonance imaging of biological specimens by electron paramagnetic resonance of nitroxide spin labels. *Science* 227: 517-519, 1985.
- Berliner LJ, Grunwald J, Hankovszky HO, and Hideg K. A novel reversible thiol-specific spin label: papain active site labeling and inhibition. *Anal Biochem* 119: 450-455, 1982.
- Berliner LJ, Khramtsov V, Fujii H, and Clanton TL. Unique in vivo applications of spin traps. *Free Radic Biol Med* 30: 489-499, 2001.
- Boyne AF and Ellman GL. A methodology for analysis of tissue sulfhydryl components. *Anal Biochem* 46: 639-653, 1972.
- Breit G and Rabi II. Measurement of nuclear spin. *Phys Rev* 38: 2082-2083, 1931.
- Brunner A, Mäder K, and Gopferich A. pH and osmotic pressure inside biodegradable microspheres during erosion. *Pharm Res* 16: 847-853, 1999.
- Bruynseels K, Gillis N, Van Hecke P, and Vanstapel F. Phosphonates as <sup>31</sup>P-NMR markers of extra- and intracellular space and pH in perfused rat liver. *NMR Biomed* 10: 263-270, 1997.
- Busse E, Zimmer G, and Kornhuber B. Plasma-membrane fluidity studies of murine neuroblastoma and malignant melanoma cells under irradiation. *Strahlenther Onkol* 168: 419-422, 1992.
- Busse E, Zimmer G, Schopohl B, and Kornhuber B. Influence of alpha-lipoic acid on intracellular glutathione in vitro and in vivo. *Arzneimittelforschung* 42: 829-831, 1992.
- Fink B, Eckes J, Fink N, and Dikalov S. Influence of HELP- and MDF-apheresis on cellular LDL-induced formation of reactive oxygen species and oxidation of extra-/intracellular SH-groups. *Free Radic Biol Med* 33: S411-S412, 2002.
- Foster MA, Grigor'ev IA, Lurie DJ, Khramtsov VV, McCallum S, Panagiotelis I, Hutchison JMS, Koptioug A, and Nicholson I. In vivo detection of a pH-sensitive nitroxide in the rat stomach by low-field ESR-based techniques. *Magn Reson Med* 49: 558-567, 2003.
- Fujii H and Berliner LJ. In vivo EPR evidence for free radical adducts of nifedipine. *Magn Reson Med* 42: 691-694, 1999.
- Gallez B, Mäder K, and Swartz HM. Noninvasive measurement of the pH inside the gut by using pH-sensitive nitroxides: an in vivo EPR study. *Magn Reson Med* 36: 694-697, 1996.
- Gallo P, Colacicchi S, Ferrari M, Gualtieri G, and Sotgiu A. Electron paramagnetic resonance spectroscopy on isolated rat heart: a technical note. *Cardioscience* 2: 221-224, 1991.
- Gillies RJ, Alger JR, den Holander JA, and Shulman RG. Intracellular pH measured by NMR: methods and results. In: *Intracellular pH: Its Measurement, Regulation and Utilization in Cellular Functions*, edited by Nuccitelli R and Deamer DW. New York: Alan R. Liss, 1982, pp. 79-104.
- Gottlieb RA, Gruol DL, Zhu JY, and Engler RL. Preconditioning in rabbit cardiomyocytes. Role of pH, vacuolar proton ATPase, and apoptosis. *J Clin Invest* 97: 2391-2398, 1996.
- Grigor'ev IA, Reznikov VA, Voinov MA, Ruuge A, and Smirnov AI. Site-directed spin-labeling with a pH-sensitive nitroxide. In: *Abstracts of Papers of 32nd South Eastern Magnetic Resonance Conference*. Raleigh, NC: North Carolina State University, 2002, p. 37.
- Hagenfeldt L, Arvidsson A, and Larsson A. Glutathione and -glutamylcysteine in whole blood, plasma and erythrocytes. *Clin Chim Acta* 85: 167-173, 1978.
- He G, Samouilov A, Kuppusamy P, and Zweier JL. In vivo imaging of free radicals: applications from mouse to man. *Mol Cell Biochem* 234-235: 359-367, 2002.
- Helmlinger G, Yuan F, Dellian M, and Jain RK. Interstitial pH and pO<sub>2</sub> gradients in solid tumors in vivo: high-resolution measurements reveal a lack of correlation. *Nat Med* 3: 177-182, 1997.
- Hubbell WL, Cafiso DS, and Altenbach C. Identifying conformational changes with site-directed spin labeling. *Nat Struct Biol* 7: 735-739, 2000.
- Ilangoan G, Li H, Zweier JL, and Kuppusamy P. In vivo measurement of tumor redox environment using EPR spectroscopy. *Mol Cell Biochem* 234-235: 393-398, 2002.
- Issberner U, Reeh PW, and Steen KH. Pain due to tissue acidosis: a mechanism for inflammatory and ischemic myalgia? *Neurosci Lett* 208: 191-194, 1996.

28. Johnson BA, Weil MH, Tang W, Noc M, McKee D, and McCandless D. Mechanisms of myocardial hypercarbic acidosis during cardiac arrest. *J Appl Physiol* 78: 1579–1584, 1995.
29. Keana JFW, Acarregui MJ, and Boyle SLM. 2,2-Disubstituted-4,4-dimethylimidazolidinyl-3-oxy nitroxides: indicators of aqueous acidity through variation of aN with pH. *J Am Chem Soc* 104: 827–830, 1982.
30. Khan N and Swartz H. Measurements in vivo of parameters pertinent to ROS/RNS using EPR spectroscopy. *Mol Cell Biochem* 234–235: 341–357, 2002.
31. Khramtsov VV. New approaches in spin labeling and spin trapping. Part one: ESR studies of local chemical environment. In: *Supramolecular Structure and Function* 7, edited by Pifat-Mrzljak G. Dordrecht, The Netherlands: Kluwer Academic/Plenum Publishers, 2001, pp. 89–105.
32. Khramtsov VV and Volodarsky LB. Use of imidazoline nitroxides in studies of chemical reactions: ESR measurements of concentration and reactivity of protons, thiols and nitric oxide. In: *Biological Magnetic Resonance, Vol. 14: Spin Labeling: The Next Millennium*, edited by Berliner LJ. New York: Plenum Press, 1998, pp. 109–180.
33. Khramtsov VV, Weiner LM, Grigor'ev IA, and Volodarsky LB. Proton exchange in stable nitroxyl radicals. EPR study of the pH of aqueous solutions. *Chem Phys Lett* 91: 69–72, 1982.
34. Khramtsov VV, Pantelev MV, and Weiner LM. ESR study of proton transport across phospholipid vesicle membranes. *J Biochem Biophys Methods* 18: 237–246, 1989.
35. Khramtsov VV, Yelinova VI, Weiner LM, Berezina TA, Martin VV, and Volodarsky LB. Quantitative determination of SH groups in low- and high-molecular weight compounds by an ESR method. *Anal Biochem* 182: 58–63, 1989.
36. Khramtsov VV, Marsh D, Weiner L, and Reznikov VA. The application of pH-sensitive spin labels to studies of surface potential and polarity of phospholipid membranes and proteins. *Biochim Biophys Acta* 1104: 317–324, 1992.
37. Khramtsov VV, Yelinova VI, Glazachev YuI, Reznikov VA, and Zimmer G. Quantitative determination and reversible modification of thiols using imidazolidine biradical disulfide label. *J Biochem Biophys Methods* 35: 115–128, 1997.
38. Khramtsov VV, Grigor'ev IA, Foster MA, Lurie DJ, and Nicholson I. Biological applications of spin pH probes. *Cell Mol Biol* 46: 1361–1374, 2000.
39. Khramtsov VV, Grigor'ev IA, Kirilyuk IA, Ilangovan G, and Kuppusamy P. In vivo EPR measurement of tissue acidosis during myocardial ischemia using pH sensitive nitroxide probes. *Free Radic Biol Med* 33(Suppl): S423–S424, 2002.
40. Kirilyuk IA, Shevelev TG, Morozov DA, Khromovskikh EL, Skuridin NG, Khramtsov VV, and Grigor'ev IA. Grignard reagent addition to 5-alkylamino-4H-imidazole 3-oxides: synthesis of new pH-sensitive spin probes. *Synthesis* No. 6, 871–878, 2003.
41. Kroll C, Mäder K, Stosser R, and Borchert HH. Direct and continuous determination of pH values in nontransparent w/o systems by means of EPR spectroscopy. *Eur J Pharmaceut Sci* 3: 21–26, 1995.
42. Kroll C, Hermann W, Stosser R, Borchert HH, and Mäder K. Influence of drug treatment on the microacidity in rat and human skin—an in vitro electron spin resonance imaging study. *Pharm Res* 18: 525–530, 2001.
43. Kuppusamy P, Chzhnan M, Wang P, and Zweier JL. Three-dimensional gated EPR imaging of the beating heart: time-resolved measurements of free radical distribution during the cardiac contractile cycle. *Magn Reson Med* 35: 323–328, 1996.
44. Kuppusamy P, Wang P, Zweier JL, Krishna MC, Mitchell JB, Ma L, Trimble CE, and Hsia CJ. Electron paramagnetic resonance imaging of rat heart with nitroxide and polynitroxyl-albumin. *Biochemistry* 35: 7051–7057, 1996.
45. Kuppusamy P, Li H, Ilangovan G, Cardounel AJ, Zweier JL, Yamada K, Krishna MC, and Mitchell JB. Noninvasive imaging of tumor redox status and its modification by tissue glutathione levels. *Cancer Res* 62: 307–312, 2002.
46. Lundberg P, Harmsen E, Ho C, and Vogel HJ. Nuclear magnetic resonance studies of cellular metabolism. *Anal Biochem* 191: 193–222, 1990.
47. Lurie DJ. Free radical imaging. *Br J Radiol* 74: 782–784, 2001.
48. Lurie DJ, Nicholson I, and Mallard JR. Low-field EPR measurements by field-cycled dynamic nuclear polarisation. *J Magn Reson* 95: 405–409, 1991.
49. Lurie DJ, Foster MA, Yeung D, and Hutchison JM. Design, construction and use of a large-sample field-cycled PEDRI imager. *Phys Med Biol* 43: 1877–1886, 1998.
50. Lurie DJ, Foster MA, Youngde W, Khramtsov VV, and Grigor'ev IA. Recent progress and future prospects of free radical imaging by PEDRI. In: *EPR in the 21st Century*, edited by Kawamori A, Yamauchi J, and Ohta H. Amsterdam: Elsevier Science BV, 2002, pp. 515–523.
51. Lurie DJ, Li H, Petryakov S, and Zweier JL. Development of a PEDRI free-radical imager using a 0.38 T clinical MRI system. *Magn Reson Med* 47: 181–186, 2002.
52. Mäder K. Pharmaceutical applications of in vivo EPR. *Phys Med Biol* 43: 1931–1935, 1998.
53. Mäder K, Gallez B, Liu KJ, and Swartz HM. Non-invasive in vivo characterization of release processes in biodegradable polymers by low-frequency electron paramagnetic resonance spectroscopy. *Biomaterials* 17: 457–461, 1996.
54. Mäder K, Nitschke S, Stosser R, and Borchert H-H. Non destructive and localized assessment of acidic microenvironments inside biodegradable polyanhydrides by spectral spatial electron paramagnetic resonance imaging. *Polymer* 38: 4785–4794, 1997.
55. Mäder K, Bittner B, Li Y, Wohlauf W, and Kissel T. Monitoring microviscosity and microacidity of the albumin microenvironment inside degrading microparticles from poly(lactide-co-glycolide) (PLG) or ABA-triblock polymers containing hydrophobic poly(lactide-co-glycolide) A blocks and hydrophilic poly(ethyleneoxide) B blocks. *Pharm Res* 15: 787–793, 1998.
56. Markel AL, Yelinova VI, and Khramtsov VV. Oxidative stress in pathogenesis of arterial hypertension in ISIAH rats. *Russ Fiziol Zh Im Sechenova* 87: 594–599, 2001.
57. Na K and Bae YH. Self-assembled hydrogel nanoparticles responsive to tumor extracellular pH from pullulan derivative/sulfonamide conjugate: characterization, aggregation,

- and adriamycin release in vitro. *Pharm Res* 19: 681–688, 2002.
58. Nicholson I, Robb FJ, McCallum SJ, Koptioug A, and Lurie DJ. Recent developments in combining LODSR imaging with proton NMR imaging. *Phys Med Biol* 43: 1851–1855, 1998.
  59. Nohl H, Stoltze K, and Weiner LM. Noninvasive measurement of thiol levels in cells and isolated organs. *Methods Enzymol* 251: 191–203, 1995.
  60. Nuccitelli R and Deamer DW (Eds). *Intracellular pH: Its Measurement, Regulation and Utilization in Cellular Functions*. New York: Alan R. Liss.
  61. Ojugo AS, McSheehy PM, McIntyre DJ, McCoy C, Stubbs M, Leach MO, Judson IR, and Griffiths JR. Measurement of the extracellular pH of solid tumours in mice by magnetic resonance spectroscopy: a comparison of exogenous  $^{19}\text{F}$  and  $^{31}\text{P}$  probes. *NMR Biomed* 12: 495–504, 1999.
  62. Pietri S, Martel S, Culcasi M, Delmas-Beauvieux M-C, Canioni P, and Gallis J-L. Use of diethyl(2-methylpyrrolidin-2-yl)phosphonate as a highly sensitive extra- and intracellular  $^{31}\text{P}$  NMR pH indicator in isolated organs. *J Biol Chem* 276: 1750–1758, 2001.
  63. Raghunand N, Howison C, Sherry AD, Zhang S, and Gillies RJ. Renal and systemic pH imaging by contrast-enhanced MRI. *Magn Reson Med* 49: 249–257, 2003.
  64. Samouilov A, Kuppusamy P, and Zweier JL. Evaluation of the magnitude and rate of nitric oxide production from nitrite in biological systems. *Arch Biochem Biophys* 357: 1–7, 1998.
  65. Schafer FQ and Buettner GR. Redox environment of the cell as viewed through the redox state of the glutathione disulfide/glutathione couple. *Free Radic Biol Med* 30: 1191–1212, 2001.
  66. Sotgiu A, Mäder K, Placidi G, Colacicchi S, Ursini CL, and Alecci M. pH-sensitive imaging by low-frequency EPR: a model study for biological applications. *Phys Med Biol* 43: 1921–1930, 1998.
  67. Szwergold BS. NMR spectroscopy of cells. *Annu Rev Physiol* 54: 775–798, 1992.
  68. Thangaraju M, Sharma K, Leber B, Andrews DW, Shen SH, and Srikant CB. Regulation of acidification and apoptosis by SHP-1 and Bcl-2. *J Biol Chem* 274: 29549–29557, 1999.
  69. Troyano A, Fernandez C, Sancho P, de Blas E, and Aller P. Effect of glutathione depletion on antitumor drug toxicity (apoptosis and necrosis) in U-937 human promonocytic cells. The role of intracellular oxidation. *J Biol Chem* 276: 47107–47115, 2001.
  70. Vandenberg JI, Metcalfe JC, and Grace A. Mechanisms of pH recovery after global ischemia in the perfused heart. *Circ Res* 72: 993–1003, 1993.
  71. Vermathen P, Capizzano AA, and Maudsley AA. Administration and  $^1\text{H}$  MRS detection of histidine in human brain: application to in vivo pH measurement. *Magn Reson Med* 43: 665–675, 2000.
  72. Villa P, Saccani A, Sica A, and Ghezzi P. Glutathione protects mice from lethal sepsis by limiting inflammation and potentiating host defense. *J Infect Dis* 185: 1115–1120, 2002.
  73. Voilley N, de Weille J, Mamet J, and Lazdunski M. Non-steroid anti-inflammatory drugs inhibit both the activity and the inflammation-induced expression of acid-sensing ion channels in nociceptors. *J Neurosci* 21: 8026–8033, 2001.
  74. Voinov M and Grigor'ev IA. New approach to the synthesis of hydrophilic pH-sensitive spin probes. In: *Abstracts of 3rd International Conference on Nitroxide Radicals*. Kaiserslautern, Germany: University of Kaiserslautern, 2001, p. 110.
  75. Weiner LM, Hu H, and Swartz HM. EPR method for the measurement of cellular sulfhydryl groups. *FEBS Lett* 290: 243–246, 1991.
  76. Xu K and Thornalley PJ. Involvement of glutathione metabolism in the cytotoxicity of the phenethyl isothiocyanate and its cysteine conjugate to human leukaemia cells in vitro. *Biochem Pharmacol* 61: 165–177, 2001.
  77. Yelinova V, Glazachev Y, Khrantsov V, Kudryashova L, Rykova V, and Salganik R. Studies of human and rat blood under oxidative stress: changes in plasma thiol level, antioxidant enzyme activity, protein carbonyl content, and fluidity of erythrocyte membrane. *Biochem Biophys Res Commun* 221: 300–303, 1996.
  78. Yelinova VI, Khrantsov VV, and Markel AL. Manifestation of oxidative stress in the pathogenesis of arterial hypertension in ISIAH rats. *Biochem Biophys Res Commun* 263: 450–453, 1999.
  79. Zweier JL, Wang P, Samouilov A, and Kuppusamy P. Enzyme-independent formation of nitric oxide in biological tissues. *Nat Med* 1: 804–809, 1995.
  80. Zweier JL, Chzhan M, Samouilov A, and Kuppusamy P. Electron paramagnetic resonance imaging of the rat heart. *Phys Med Biol* 43: 1823–1835, 1998.

Address reprint requests to:

Valery V. Khrantsov

Dorothy M. Davis Heart & Lung Research Institute

The Ohio State University

Columbus, OH 43210

E-mail: khrantsov-1@medctr.osu.edu

Received for publication July 8, 2003; accepted February 19, 2004.

**This article has been cited by:**

1. Igor A. Kirilyuk, Yuliya F. Polienko, Olesya A. Krumkacheva, Rodion K. Strizhakov, Yurii V. Gatilov, Igor A. Grigor'ev, Elena G. Bagryanskaya. 2012. Synthesis of 2,5-Bis(spirocyclohexane)-Substituted Nitroxides of Pyrroline and Pyrrolidine Series, Including Thiol-Specific Spin Label: An Analogue of MTSSL with Long Relaxation Time. *The Journal of Organic Chemistry* **77**:18, 8016-8027. [[CrossRef](#)]
2. Yangping Liu, Yuguang Song, Antal Rockenbauer, Jian Sun, Craig Hemann, Frederick A. Villamena, Jay L. Zweier. 2011. Synthesis of Trityl Radical-Conjugated Disulfide Biradicals for Measurement of Thiol Concentration. *The Journal of Organic Chemistry* **76**:10, 3853-3860. [[CrossRef](#)]
3. Olga V. Efimova, Ziqi Sun, Sergey Petryakov, Eric Kesselring, George L. Caia, David Johnson, Jay L. Zweier, Valery V. Khramtsov, Alexandre Samouilov. 2011. Variable radio frequency proton-electron double-resonance imaging: Application to pH mapping of aqueous samples. *Journal of Magnetic Resonance* **209**:2, 227-232. [[CrossRef](#)]
4. A. A. Bobko, I. A. Kirilyuk, N. P. Gritsan, D. N. Polovyanenko, I. A. Grigor'ev, V. V. Khramtsov, E. G. Bagryanskaya. 2010. EPR and Quantum Chemical Studies of the pH-sensitive Imidazoline and Imidazolidine Nitroxides with Bulky Substituents. *Applied Magnetic Resonance* **39**:4, 437-451. [[CrossRef](#)]
5. Valery V. Khramtsov, Jay L. Zweier Functional in vivo EPR Spectroscopy and Imaging Using Nitroxide and Trityl Radicals 537-566. [[CrossRef](#)]
6. Hakim Karoui, François Le Moigne, Olivier Ouari, Paul Tordo Nitroxide Radicals: Properties, Synthesis and Applications 173-229. [[CrossRef](#)]
7. Sergey Petryakov, Alexandre Samouilov, Eric Kesselring, George L. Caia, Ziqi Sun, Jay L. Zweier. 2010. Dual frequency resonator for 1.2GHz EPR/16.2MHz NMR co-imaging. *Journal of Magnetic Resonance* **205**:1, 1-8. [[CrossRef](#)]
8. Nadeem Khan , Valery V. Khramtsov , Harold M. Swartz Methods for Tissue pO<sub>2</sub>, Redox, pH, and Glutathione Measurements by EPR Spectroscopy 81-89. [[Abstract](#)] [[Summary](#)] [[Full Text PDF](#)] [[Full Text PDF with Links](#)]
9. Sergey Petryakov, Alexandre Samouilov, Michael Chzhzhan-Roytenberg, Eric Kesselring, Ziqi Sun, Jay L. Zweier. 2009. Segmented surface coil resonator for in vivo EPR applications at 1.1GHz. *Journal of Magnetic Resonance* **198**:1, 8-14. [[CrossRef](#)]
10. Yakov Y. Woldman, Sergey V. Semenov, Andrey A. Bobko, Igor A. Kirilyuk, Julya F. Polienko, Maxim A. Voinov, Elena G. Bagryanskaya, Valery V. Khramtsov. 2009. Design of liposome-based pH sensitive nanoSPIN probes: nano-sized particles with incorporated nitroxides. *The Analyst* **134**:5, 904. [[CrossRef](#)]
11. Aditi C. Kulkarni, Anna Bratasz, Brian Rivera, Murali C. Krishna, Periannan Kuppusamy. 2008. Redox Mapping of Biological Samples Using EPR Imaging. *Israel Journal of Chemistry* **48**:1, 27-31. [[CrossRef](#)]
12. Galina I. Roshchupkina, Andrey A. Bobko, Anna Bratasz, Vladimir A. Reznikov, Periannan Kuppusamy, Valery V. Khramtsov. 2008. In vivo EPR measurement of glutathione in tumor-bearing mice using improved disulfide biradical probe. *Free Radical Biology and Medicine* **45**:3, 312-320. [[CrossRef](#)]
13. E. V. Fomenko, A. A. Bobko, A. N. Salanov, I. A. Kirilyuk, I. A. Grigor'ev, V. V. Khramtsov, A. G. Anshits. 2008. Perforated cenosphere-supported pH-sensitive spin probes. *Russian Chemical Bulletin* **57**:3, 493-498. [[CrossRef](#)]
14. Harold M. Swartz , Nadeem Khan , Valery V. Khramtsov . 2007. Use of Electron Paramagnetic Resonance Spectroscopy to Evaluate the Redox State In Vivo. *Antioxidants & Redox Signaling* **9**:10, 1757-1772. [[Abstract](#)] [[Full Text PDF](#)] [[Full Text PDF with Links](#)]
15. D POTAPENKO, M FOSTER, D LURIE, I KIRILYUK, J HUTCHISON, I GRIGOREV, E BAGRYANSKAYA, V KHRAMTSOV. 2006. Real-time monitoring of drug-induced changes in the

stomach acidity of living rats using improved pH-sensitive nitroxides and low-field EPR techniques. *Journal of Magnetic Resonance* **182**:1, 1-11. [[CrossRef](#)]

16. Dmitrii I. Potapenko, Elena G. Bagryanskaya, Igor A. Grigoriev, Aleksander M. Maksimov, Vladimir A. Reznikov, Vyacheslav E. Platonov, Thomas L. Clanton, Valery V. Khramtsov. 2005. Quantitative determination of SH groups using  $^{19}\text{F}$  NMR spectroscopy and disulfide of 2,3,5,6-tetrafluoro-4-mercaptobenzoic acid. *Magnetic Resonance in Chemistry* **43**:11, 902-909. [[CrossRef](#)]
17. Igor A. Kirilyuk, Andrey A. Bobko, Valery V. Khramtsov, Igor A. Grigor'ev. 2005. Nitroxides with two pK values? useful spin probes for pH monitoring within a broad range. *Organic & Biomolecular Chemistry* **3**:7, 1269. [[CrossRef](#)]
18. Periannan Kuppusamy . 2004. EPR Spectroscopy in Biology and Medicine. *Antioxidants & Redox Signaling* **6**:3, 583-585. [[Citation](#)] [[Full Text PDF](#)] [[Full Text PDF with Links](#)]
19. Dipak K. Das Methods in Redox Signaling . [[Citation](#)] [[Full Text HTML](#)] [[Full Text PDF](#)] [[Full Text PDF with Links](#)]